Int J Legal Med (2011) 125:549–558
DOI 10.1007/s00414-011-0567-4

ORIGINAL ARTICLE

Time-dependent expression and distribution of monoacylglycerol lipase during the skin-incised wound healing in mice

Wen-Xiang Ma · Tian-Shui Yu · Yan-Yan Fan · Shu-Tao Zhang · Peng Ren · Shuai-Bo Wang · Rui Zhao · Jing-Bo Pi · Da-Wei Guan

Received: 4 November 2010 / Accepted: 14 February 2011 / Published online: 8 April 2011

Abstract The study investigated the expression of monoacylglycerol lipase (MGL) during the skin-incised wound healing in mice and applicability of the time-dependent expression of MGL to wound age determination by immunofluorescent staining, Western blotting, and real-time PCR. Furthermore, cell types were identified by double immunofluorescence. A total of 45 BALB/c male mice were used in this study. After a 1.5-cm-long incision in the central dorsum skin, mice were killed at intervals ranging from 6 h to 14 days, followed by the sampling of wound margin. In the control, there was a low-level expression of MGL in the epidermis, hair follicles, and glandulae sebaceae. In the injured skin, MGL immunoreactivity was mainly detected in the neutrophils, macrophages, and myofibroblasts. Morphometrically, the average ratios of MGL-positive cells were more than 50% at 5 and 7 days post-wounding, whereas it was <50% at the other posttraumatic intervals. By Western blotting analysis, the average ratio of MGL protein expression was highest at 5 days after injury, which had a ratio of >2.30. Similarly, the relative quantity of MGL mRNA expression maximized at posttraumatic 5 days in comparison with control as detected by real-time PCR, with an average ratio of >2.54. In conclusion, MGL expression is detected in neutrophils, macrophages, and myofibroblasts and significantly up-regulated, suggesting that it may play roles in response to inflammation during skin-incised wound healing. From the viewpoint of forensic pathology, MGL detection is applicable to skin wound age determination.

Keywords Wound age determination · Skin wound · MGL · Macrophage · Myofibroblast · Real-time PCR

W.-X. Ma · T.-S. Yu · Y.-Y. Fan · S.-T. Zhang · P. Ren · S.-B. Wang · R. Zhao · D.-W. Guan (✉)
Department of Forensic Pathology,
China Medical University School of Forensic Medicine,
No.92, Beier Road, Heping District,
Shenyang, Liaoning Province 110001,
People's Republic of China
e-mail: dwguan@mail.cmu.edu.cn

D.-W. Guan
e-mail: dwguan007@yahoo.com.cn

J.-B. Pi
Division of Translational Biology,
The Hamner Institutes for Health Sciences,
Research Triangle Park, NC 27709, USA

Introduction

It is generally acknowledged that endogenous cannabinoid system is ubiquitous in mammals. Moreover, it is evidenced that the system is involved in a wide spectrum of physiological and pathological events. Unlike other transmitters, endocannabinoids are synthesized and released "on demand". Endocannabinoid levels appear to be transiently elevated as an adaptive reaction to reestablish normal homeostasis when it is perturbed [1, 2]. This system is composed of cannabinoid receptor (CB1 receptor and CB2 receptor), endogenous ligands (endocannabinoids), and enzymes that synthesize and degrade endocannabinoids. Currently, three enzymes have been characterized with the ability to hydrolyze endocannabinoids: fatty acid amide hydrolase (FAAH), monoacylglycerol lipase (MGL), and *N*-acylethanolamine-hydrolyzing acid amidase [3]. Originally, MGL was purified and cloned from mouse adipose tissue in 1977, where it catalyzed the final step of triglyceride metabolism. MGL

is a member of the serine hydrolase family and now considered as one of the most important endocannabinoid hydrolases, which is the primary enzyme metabolizing 2-arachidonoylglycerol (2-AG) [4, 5].

Skin wound healing is a complicated but well-controlled sequential biological process. It is well established that skin wound healing can be temporally divided into three phases, the early acute exudative, fibro-proliferative, and tissue remodeling phases. During the early acute exudative phase, various types of inflammatory cells such as neutrophils and macrophages are recruited at the wound site. These cells eradicate microbes and provide cytokines and growth factors. Subsequently, in the proliferative phase, myofibroblasts migrate to the wound area and proliferate to repair tissue destruction [6, 7]. There is increasing evidence that a variety of cytokines, growth factors, and chemokines are involved in skin wound healing process [8–12]. Recently, MGL expression in various mouse organs is examined by Western blotting [4]. It has been documented that MGL is expressed at high levels in the rodent brain, where it is predominantly found in presynaptic nerve terminals of both excitatory and inhibitory neurons [13, 14]. Hitherto, there is no research reported on MGL during the skin-incised wound healing. With respect to the inflammation, URB602 (1-1′ biphenyl-3-ylcarbamic acid cyclohexyl ester), a selective inhibitor of MGL, has a dose-dependent action in reducing not only edema but also thermal hypersensitivity associated with inflammation by the selective enhancement of 2-AG and enhances stress-induced analgesia in a CB1-dependent manner [15–17]. Moreover, it is demonstrated that URB602 induces anti-allodynic and anti-nociceptive effects in a rat model of neuropathic pain [18]. Besides, data mining via the GEO database (www.ncbi.nlm.nih.gov/geo/) reveals that fibroblasts, myofibroblasts, chondrocytes, and synoviocytes express endocannabinoid ligand-metabolizing enzymes [19]. Based on studies mentioned above, it is presumed that MGL may be involved in inflammatory reactions after skin injury.

In the present study, we investigated the expression and distribution of MGL at different posttraumatic intervals during the skin-incised wound healing in mice. Meanwhile, attempt was made for MGL as a possible marker for wound age estimation.

Materials and methods

Animal model of the incised skin wound

Establishment of an animal model for an incised skin wound was described previously [8]. Briefly, a total of 45 male adult healthy BALB/c mice, each weighing 35–40 g, were employed. Forty mice were anesthetized by intraperitoneal injection with sodium pentobarbital. Subsequently, a 1.5-cm-long incision was made with a scalpel in the skin layer on the central dorsum under sterile technique. After incision was made, each mouse was individually housed in a cage and fed with commercial mouse chow and distilled water to prevent bacterial infection. All mice were kept under a 12-h light–dark cycle with specific pathogen-free conditions during the experiments. After the animals were killed by cervical dislocation after anaesthetization at 6 h, 12 h, 1 day, 3 days, 5 days, 7 days, 10 days, and 14 days post-injury (five mice at each posttraumatic interval), 1.5× 1-cm specimens were taken from wounded sites. One half of each specimen was used for immunofluorescent procedure, and another was used for Western blotting and real-time PCR. The remaining five mice were anesthetized without incision as controls.

Experiments conformed to the "Principles of Laboratory Animal Care" (National Institutes of Health publication no. 85-23, revised 1985) that sought to minimize both the number of animals used and any suffering that they might experience, and were performed according to the Guidelines for the Care and Use of Laboratory Animals of China Medical University.

Tissue preparation and immunofluorescent staining

The skin specimens were immediately fixed in 4% paraformaldehyde/0.1 M phosphate-buffered saline (PBS, pH 7.4) for 12 h, and then specimens were washed in tap water and distilled water. The skins were immersed in 10% and 20% sucrose 0.1 M PBS for 12 h at 4°C, respectively, and 30% sucrose 0.1 M PBS at 4°C until they sank at the bottom of the container. The specimens were embedded in OCT and 5-μm-thick serial sections were prepared. Briefly, following a rinse in PBS, the sections were blocked with 5% bovine serum albumin (BSA) to reduce nonspecific reactions and incubated with rabbit anti-MGL polyclonal antibody (dilution 1:100; ab24701, Abcam, Cambridge, UK) overnight at 4°C. Thereafter, the sections were further incubated with Rhodamine (TRITC)-AffiniPure goat anti-rabbit IgG (dilution 1:150; 111-025-045, Jackson Immunoresearch, PA, USA) at room temperature for 2 h and the nuclei routinely counterstained with Hoechst 33258. As controls for immunofluorescent procedures, some sections were incubated with PBS or normal rabbit IgG in place of the primary antibody. The sections were observed under a fluorescence microscope with Digital CCD Imaging System (BX61/DP71, Olympus, Japan). Meanwhile, the sections were routinely stained with hematoxylin–eosin. For cell count, only cells (except epidermis, hair follicles, and glandulae sebaceae cells) infiltrated into the peripheral zone of the wound and wound cavity were recruited. In each

section, ten microscopic fields at 400-fold magnification were randomly selected, and the ratio of MGL-positive cells to the total number of cells was calculated in each microscopic field. The average ratio of the ten selected microscopic fields was evaluated in each wound specimen and expressed as percentage. Two forensic pathologists independent of the experiments were responsible for cell counting and data analysis.

Double direct and indirect immunofluorescence

Briefly, the sections were blocked with 5% BSA and incubated with rabbit anti-MGL polyclonal antibody (dilution 1:100; ab24701, Abcam) at room temperature for 2 h. Thereafter, tissue sections were further incubated with Rhodamine (TRITC)-AffiniPure goat anti-rabbit IgG (dilution 1:100; 111-025-045, Jackson Immunoresearch) at room temperature for 2 h. Then, the sections were incubated with rabbit anti-myeloperoxidase (MPO) polyclonal antibody (dilution 1:100; sc-33596, Santa Cruz Biotechnology, CA, USA) overnight at 4°C after blocking with 5% BSA. After incubation with FITC-AffiniPure goat anti-rabbit IgG (dilution 1:100; 111-095-045, Jackson Immunoresearch) at room temperature for 2 h, the nuclei were counterstained with Hoechst 33258. Normal rabbit IgG or PBS was used instead of primary antibody as negative control.

The sections were blocked with 5% BSA and incubated with rabbit anti-MGL polyclonal antibody (dilution 1:100; ab24701, Abcam) and rat anti-macrophage marker (F4/80) monoclonal antibody (dilution 1:50; sc-52664, Santa Cruz Biotechnology) overnight at 4°C. Then, the sections were incubated with Rhodamine (TRITC)-AffiniPure Goat anti-Rabbit IgG (dilution 1:100; 111-025-045, Jackson Immunoresearch) and Alexa Fluor® 488 donkey anti-rat IgG (dilution 1:100; A21202, Invitrogen, CA, USA) at room temperature for 2 h and the nuclei counterstained with Hoechst 33258. Normal rabbit or rat IgG was used instead of primary antibodies as negative control.

The sections were blocked with 10% non-immune goat serum to reduce nonspecific binding. Then, tissue sections were incubated with rabbit anti-MGL polyclonal antibody (dilution 1:100; ab24701, Abcam) at room temperature for 2 h. The sections were further incubated with biotinylated donkey anti-rabbit IgG (dilution 1:150; ab6801, Abcam) and streptavidin, Alexa Fluor® 555 conjugate (dilution 1:200; S-21381, Invitrogen). Then, tissue sections were incubated with rabbit anti-α-smooth muscle actin (α-SMA) polyclonal antibody (dilution 1:50; ab5694, Abcam) overnight at 4°C after blocking with 5% BSA. After incubation with FITC-AffiniPure goat anti-rabbit IgG (dilution 1:100; 111-095-045, Jackson Immunoresearch) at room temperature for 2 h, the nuclei were counterstained with Hoechst 33258. Normal rabbit IgG or PBS was used instead of primary antibody as negative control. The sections were observed under a fluorescence microscope with Digital CCD Imaging System.

For positive cell ratio evaluation, in each section, ten microscopic fields at 400-fold magnification were randomly selected in the peripheral zone of the wound and wound cavity, and the ratio of MGL-positive cells to the total number of cells in each positive cell type was calculated in each microscopic field. The average ratio of the ten selected microscopic fields was evaluated in each wound specimen and expressed as percentage.

Protein preparation and immunoblotting assay

The skin samples were diced into very small pieces using a clean razor blade and homogenized with a homogenizer in RIPA buffer (sc-24948, Santa Cruz Biotechnology) containing protease inhibitors at 4°C. Homogenates were centrifuged at 12,000×*g* for 30 min at 4°C three times and the resulting supernatants collected. Protein concentrations were determined by BCA method. Aliquots of the supernatants were diluted in an equal volume of 5× electrophoresis sample buffer and boiled for 5 min. Protein lysates (50 μg) were separated on a 12% sodium dodecyl sulfate polyacrylamide electrophoresis gel and transferred onto polyvinylidene fluoride membranes (Millipore, Billerica, MA, USA). Nonspecific binding was blocked with Tris-buffered saline containing 5% nonfat dry milk at room temperature for 1.5 h. Then, the blots were probed with rabbit anti-MGL polyclonal antibody (dilution 1:300; ab24701, Abcam) at 4°C overnight. After washing with Tris-buffered saline buffer containing Tween#20, the membranes were incubated with horseradish peroxidase-conjugated goat anti-rabbit IgG (dilution 1:3000; sc-2004,

Table 1 Real-time PCR primer sequences

Gene	GenBank ID	Species	Primer		Position	Product size (bp)
MGL	NM_011844	mouse	Forward	5′-TGA TTT CAC CTC TGG TCC TTG-3′	802–822	146
			Reverse	5′-GTC AAC CTC CGA CTT GTT CC-3′	928–947	
β-actin	NM_007393	Mouse	Forward	5′-ACC TTC TAC AAT GAG CTG CG-3′	344–363	147
			Reverse	5′-CTG GAT GGC TAC GTA CAT GG-3′	471–490	

Santa Cruz Biotechnology) at room temperature for 3 h. The blots were visualized with Western blotting luminol reagent (sc-2048, Santa Cruz Biotechnology) by Electrophoresis Gel Imaging Analysis System (MF-ChemiBIS 3.2, DNR Bio-Imaging Systems, ISR). Subsequently, densitometric analyses of the bands were semi-quantitatively conducted using Scion Image Software (Scion Corporation, MD, USA). The relative protein levels were calculated by comparison with the amount of β-actin (A03-60BM, SignalChem, Canada) as a loading control.

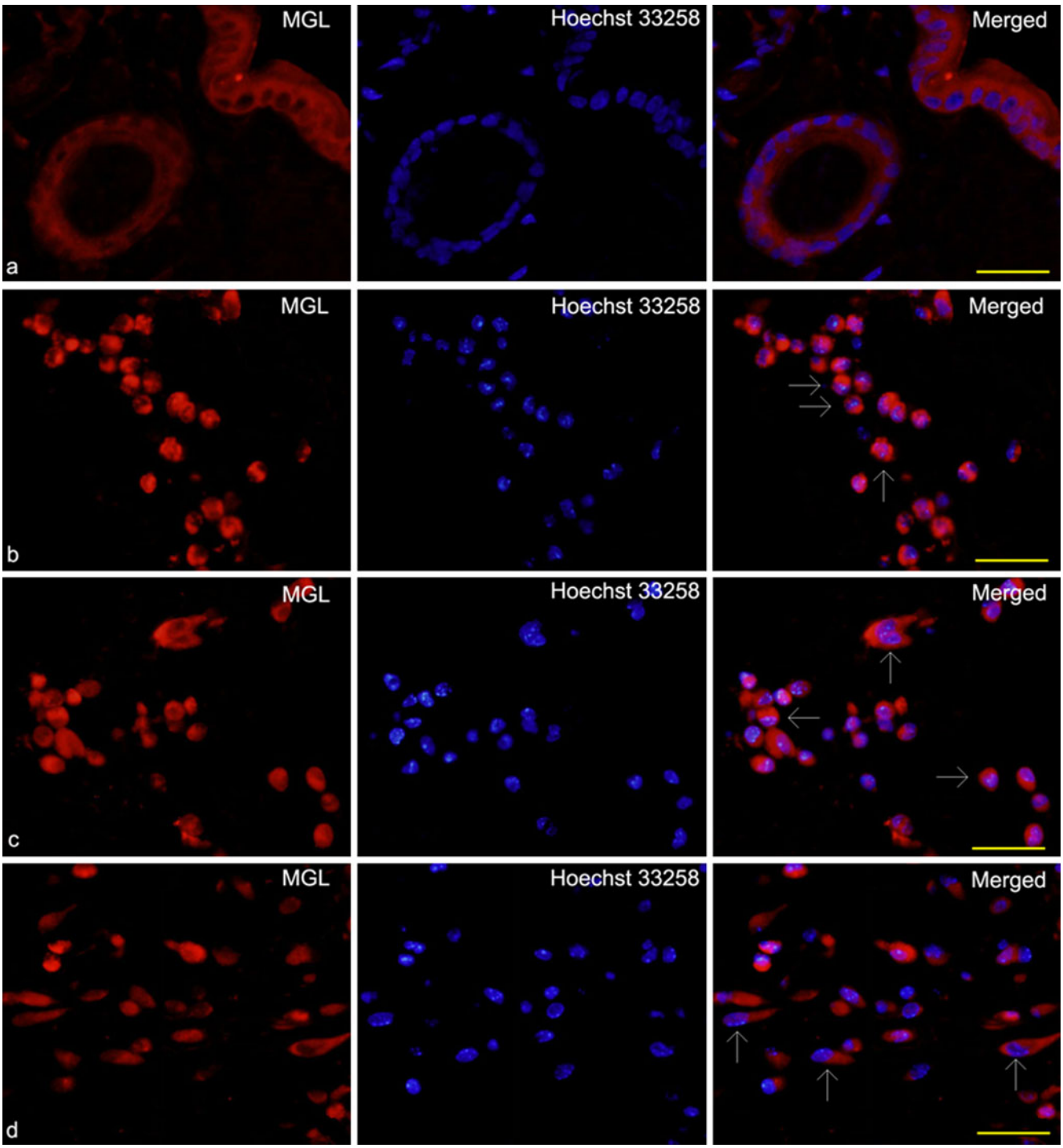

Fig. 1 Immunofluorescent staining of MGL in mouse skin wound. The samples are immunostained with anti-MGL (*red*) and Hoechst 33258 (*blue*). **a** MGL immunoreactivity is found in epidermis, hair follicles, and glandulae sebaceae in the normal mouse skin. **b** MGL-positive PMNs (*arrows*) are detected in the area of wound at 12 h post-wounding. **c**, **d** Round-shaped MNCs (*arrows*) and spindle-shaped FBCs (*arrows*) are positively immunostained in the area of wound at 3 and 7 days after injury. *Scale bars*, 50 μm

Table 2 Average ratio of MGL-positive cells in different periods

Group	Positive cells ratio (%)
Control	9.17±0.75*
6 h	30.79±2.18**
12 h	42.27±1.81**
1 day	32.16±2.27**
3 days	40.21±1.36**
5 days	54.72±1.64**
7 days	51.92±2.02**
10 days	31.58±2.12**
14 days	19.93±1.05**

*$p<0.01$ (vs. each posttraumatic interval); **$p<0.05$ (vs. preceding posttraumatic interval)

Real-time fluorescent quantitative PCR

Total RNA was isolated from the skin specimens (weight 100 mg) by use of RNAiso Plus (9108, Takara Biotechnology, Shiga, Japan) according to the manufacturer's instructions. The RNA pellet was air-dried for 5 min and resuspended in 30 μl diethylpyrocarbonate-treated dH_2O. OD values for each RNA sample were measured by ultraviolet spectrophotometer. A260/A280 ranged from 1.8 to 2.0. Using 1 μg of total RNA, 28S, 18S, and 5.8S (5S) rRNA were observed clearly by agarose gel electrophoresis. The RNA was reversely transcribed into cDNA using PrimeScript™ RT reagent Kit (RR037A, Takara Biotechnology). cDNA synthesis was performed in a 20-μl reaction mixture containing 11 μl RNase-free dH_2O, 4 μl 5× Prime Buffer, 1 μl Oligo dT, 1 μl Random 6 mers, 1 μl RT Enzyme MixI, and 1 μg of total RNA. The resulting cDNA was used for real-time PCR with the sequence-specific primer pairs for MGL and β-actin (Table 1). Real-time PCR amplification used SYBR® PrimeScript™ RT-PCR Kit (RR081A, Takara Biotechnology). Aliquots of 20-μl reaction mixture contained 6.8 μl dH_2O, 10 μl SYBR® *Premix Ex Taq*™ (2×), 0.4 μl PCR forward primer (10 μM), 0.4 μl PCR reverse primer (10 μM), 0.4 μl ROX Reference Dye II (50×) *3, and 2 μl cDNA. Amplification was performed by one round of predenaturation at 95°C for 30 s, step cycle mode of 40 rounds of denaturation at 95°C for 5 s, and annealing and extension at 60°C for 34 s by Applied Biosystems 7500 Real-Time PCR System using a 96-well optical reaction plate. To exclude any potential contamination, negative controls were also performed with dH_2O instead of cDNA during each run. No amplification product was detected. The real-time PCR procedure was repeated at least three times for each sample.

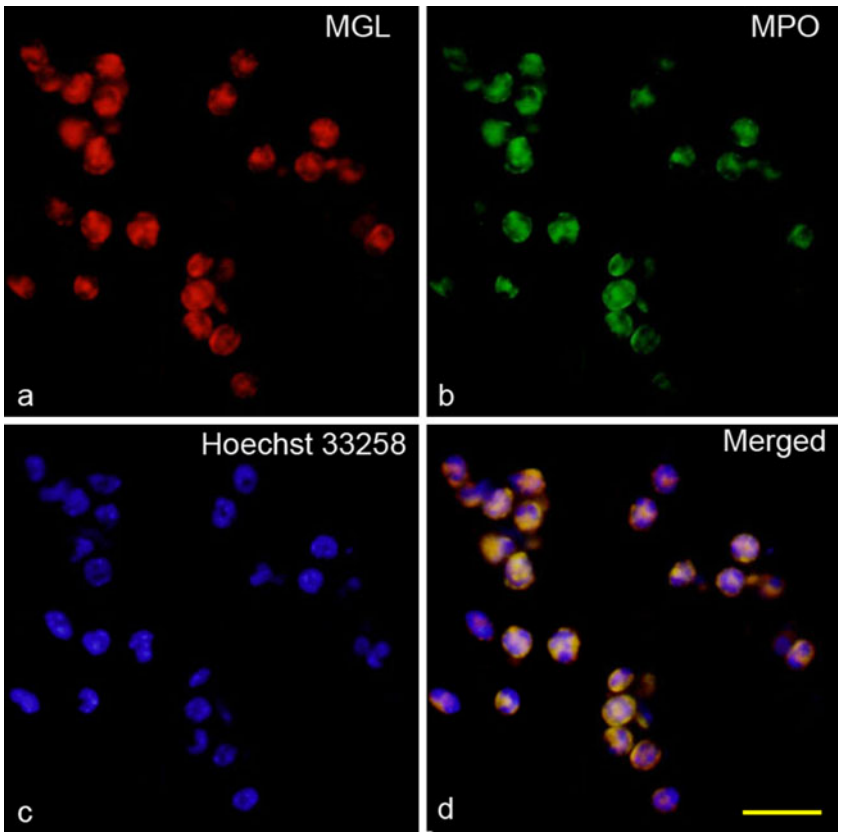

Fig. 2 A double-color immunofluorescence analysis is performed to determine MGL-expressing neutrophils at 12 h post-injury. The samples are immunostained with anti-MGL (**a**) (*red*) and anti-MPO (**b**) (*green*). Nuclei are counterstained with Hoechst 33258 (**c**) (*blue*). Co-localization of MGL and neutrophils are shown in digitally merged image (**d**) (*yellow*). Representative results from five individual experiments are shown here. *Scale bars*, 50 μm

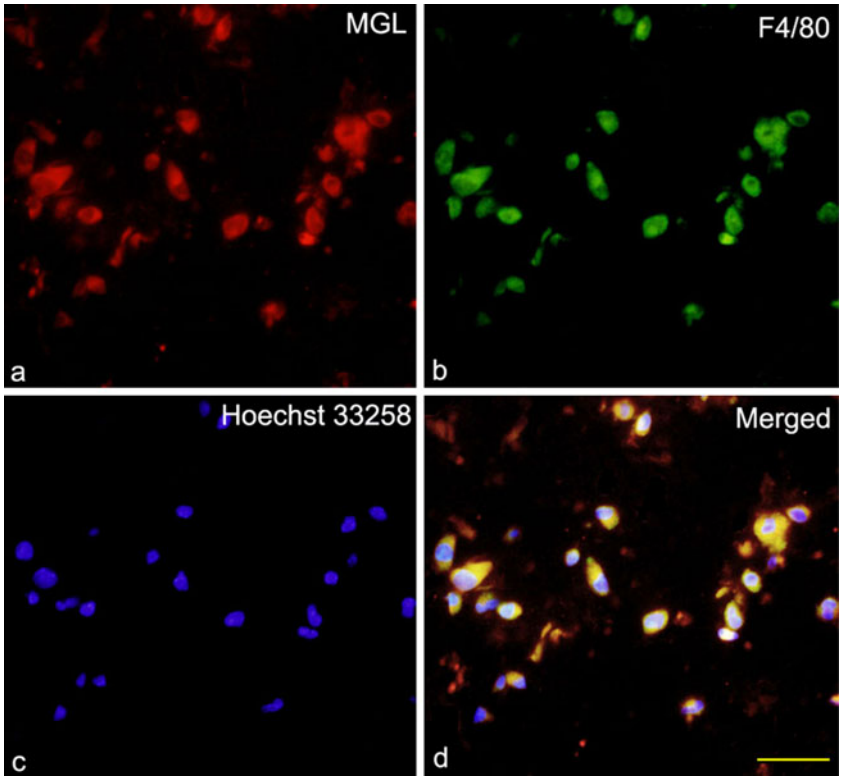

Fig. 3 Double immunofluorescence analysis is performed to determine MGL-expressing macrophages at 3 days post-injury. The samples are immunostained with anti-MGL (**a**) (*red*) and anti-F4/80 (**b**) (*green*). Nuclei are counterstained with Hoechst 33258 (**c**) (*blue*). Co-localization of MGL and macrophages are shown in digitally merged image (**d**) (*yellow*). Representative results from at least three individual experiments are shown here. *Scale bars*, 50 μm

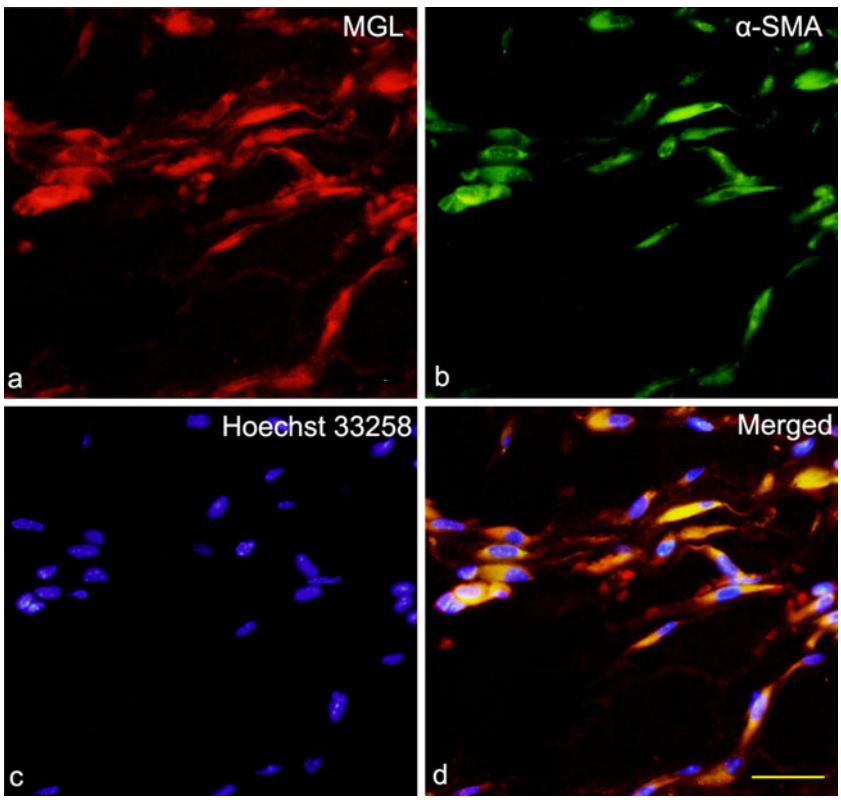

Fig. 4 Double-color immunofluorescence analysis is performed to determine MGL-expressing myofibroblasts at 7 days post-wounding. The samples are immunostained with anti-MGL (**a**) (*red*) and anti-α-SMA (**b**) (*green*). Nuclei are counterstained with Hoechst 33258 (**c**) (*blue*). Co-localization of MGL and myofibroblasts are shown in digitally merged image (**d**) (*yellow*). Representative results from five individual experiments are shown here. *Scale bars*, 50 μm

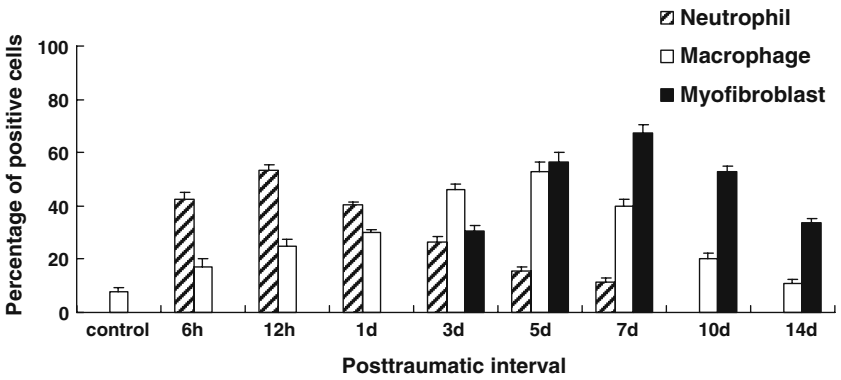

Fig. 5 Average ratios of MGL-positive neutrophils, macrophages, and myofibroblasts in relation to wound age. $p \leq 0.05$ (between two adjacent posttraumatic intervals)

Statistical analysis

Data were expressed as means±SD. For Western blot or real-time PCR data, comparison was made between two adjacent posttraumatic intervals and analyzed using SPSS for Windows 13.0. One-way ANOVA was used for data analysis. A value of $p<0.05$ was considered as statistically significant.

Results

Immunofluorescent examination

In the normal mouse skin, positive expression of MGL was weakly detected in the epidermis, hair follicles, and glandulae sebaceae (Fig. 1a). In the injured skin, MGL was positive in polymorphonuclear cells (PMNs) aged from 6 h to 1 day after injury (Fig. 1b). Afterwards, MGL-positive staining was observed in round-shaped mononuclear cells (MNCs; Fig. 1c) and spindle-shaped fibroblastic cells (FBCs; Fig. 1d) in the wound zones. Morphometrically, the average ratios of MGL-positive cells to total cells were over 50% at 5 and 7 days post-wounding, whereas it was <50% at the other posttraumatic intervals (Table 2). No false-positive staining was detected in the sections used as controls for immunofluorescent procedures.

For the identification of PMNs, co-localization of MGL and MPO were conducted by double indirect immunofluorescent method. In the control, no MGL^+/MPO^+ cells were observed. At 12 h post-injury, a large quantity of PMNs infiltrated into the injured site showed MGL^+/MPO^+ (Fig. 2). After 3 days post-injury, the number of double-positive cells reduced at the wound zones.

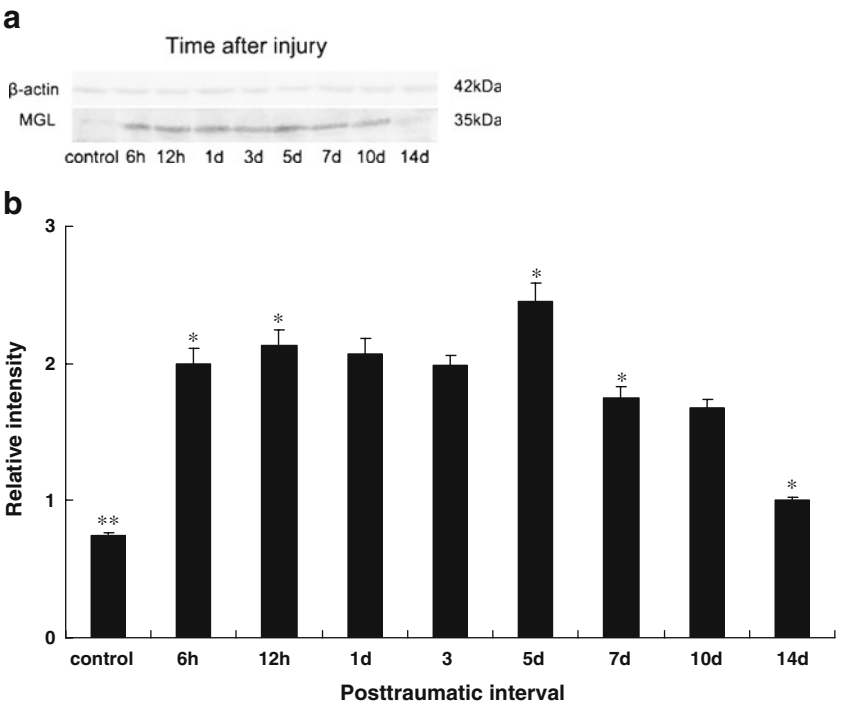

Fig. 6 **a** Analysis of MGL and β-actin protein from skin specimens by Western blotting. Representative results from five individual animals are shown. **b** Relative intensity of MGL to β-actin. All values are expressed as the means±SEM ($n=5$). *$p<0.05$ (vs. preceding posttraumatic interval); **$p<0.01$ (vs. each posttraumatic interval)

For the identification of MNCs, co-localization of MGL and F4/80 were conducted by double direct immunofluorescent method. In the control, a few of the $MGL^+/F4/80^+$ cells were observed in the dermal layer. At 3 days post-injury, a large number of MNCs infiltrated into the injured site showed $MGL^+/F4/80^+$ (Fig. 3). From 7 days post-injury, less double-positive cells were detected at the wound zones.

For the identification of FBCs, co-localization of MGL and α-SMA were conducted by double indirect immunofluorescent method. At 1 day post-injury, a few of $MGL^+/\alpha\text{-SMA}^+$ cells appeared in the wound sites. With extension of posttraumatic interval, a lot of $MGL^+/\alpha\text{-SMA}^+$ cells were noted (Fig. 4). After 10 days post-injury, $MGL^+/\alpha\text{-SMA}^+$ cells decreased in number gradually.

Meanwhile, the average ratios of MGL-positive neutrophils, macrophages, and myofibroblasts were evaluated (Fig. 5). In each positive cell type, there was a significant difference between two adjacent posttraumatic intervals.

Western blotting

The blots against MGL and β-actin antibody were shown in Fig. 6a. The average ratio of MGL protein expression peaked at 5 days after incision, which was >2.30. MGL protein expression was increased nearly twofold as early as 6 h and decreased from 7 days after injury. Significant differences in the relative expression levels of MGL protein were noted between control and each posttraumatic interval. There were significant differences in the relative intensity of MGL to β-actin between 6 and 12 h, or 3 and 5 days, or 5 and 7 days, or 10 and 14 days after injury (Fig. 6b).

Real-time fluorescent quantitative PCR

Relative quantity of MGL mRNA expression in mouse skin was assayed by real-time PCR throughout the 14 days after incision. The dissociation curves of β-actin and MGL genes showed signal cusps, and the dissociation temperatures were 87°C and 86°C, respectively. The mean ratios of MGL mRNA expression reached peak levels at 6 h and 5 days after injury as compared with that in the control. The ratio of MGL mRNA expression at 5 days post-injury was more than 2.54, whereas it was <2.54 at the other posttraumatic intervals. Significant differences in the relative quantity of MGL mRNA expression were observed between control and each posttraumatic interval. There were significant differences in the relative quantity of MGL mRNA expression between 6 and 12 h, or 12 h and 1 day, or 1 and 3 days, or 3 and 5 days, or 5 and 7 days, or 10 and 14 days after injury (Fig. 7).

Discussion

Skin wound healing requires a complex interaction of different cell types and regulation by various cytokines and bioactive molecules [20]. It is generally accepted that skin damage induces massive inflammatory cell infiltration into injured zones, including neutrophils, macrophages, and myofibroblasts [21]. Our present study, for the first time, revealed that MGL-positive staining was observed in the cytoplasm of neutrophils, macrophages, and myofibroblasts of skin-injured zones. In the endogenous cannabinoid system, MGL is mainly hydrolyzing 2-AG, an endogenous ligand for the cannabinoid receptors. At present, with respect to 2-AG physiological role in inflammation, controversial findings have been reported. Some studies suggest that 2-AG and CB2 receptor play crucial stimulative roles in different types of inflammatory and immune reactions [22]. In contrast, several investigators report that 2-AG attenuates both inflammatory reactions and immune responses [23]. Moreover, it is considered that 2-AG, rather than anandamide, is the true natural ligand for the

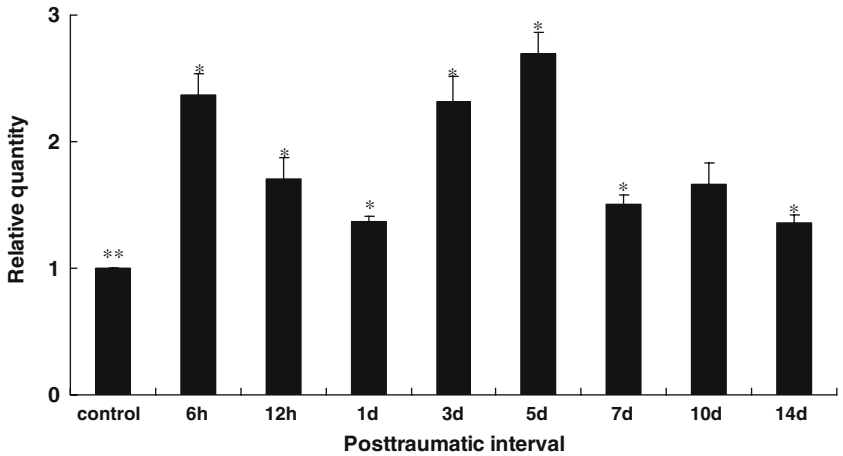

Fig. 7 Relative quantity of MGL mRNA expression. All values are expressed as the means±SEM (n=5). *p<0.05 (vs. preceding posttraumatic interval); **p<0.01 (vs. each posttraumatic interval)

cannabinoid receptors, especially CB2 receptor [24]. According to our previous study, CB2 receptor is expressed in PMNs, macrophages, FBCs, contused skeletal muscle fibers, and regenerated multinucleated myotubes and is involved in the inflammatory response of macrophages in rat skeletal muscle wound healing [25]. Our present data demonstrated that MGL expression was significantly up-regulated, suggesting that it may be involved in response to inflammation during the skin-incised wound healing. Besides, the study of stimulus-induced biosynthesis and the inactivation of 2-AG by circulating and tumoral macrophages indicate that macrophages play an important role in the homeostasis of endocannabinoids through metabolic mechanisms, including the hydrolysis of MGL and FAAH [26]. In addition, MGL is also expressed in astrocytes, which hydrolyzes 2-AG and finely tunes its production [27]. It may therefore be assumed that MGL expressed by neutrophils, macrophages, and myofibroblasts play essential roles in the maintenance of 2-AG levels during the skin wound healing in mice.

Conventionally, most of the studies regarding wound age determination in skin were conducted by histopathology and immunohistochemistry. Nowadays, attempt has been made for timing of wound by detection of mRNA [28]. Recently, analysis of mRNA expression in ten genes using real-time PCR implies that genes have differential expressional patterns with time course in mouse skin wound [29]. The time-dependent expression of troponin I mRNA in the contused skeletal muscle of rats was detected by real-time PCR for wound age estimation [30]. From the viewpoint of application of our data to forensic practice, MGL-positive ratios of >50% possibly indicate a wound age of 5–7 days as detected by immunofluorescent analysis. Moreover, the expression levels of three types of cells increased in a time-dependent manner after the wounds were inflicted. The ratio of MGL-positive neutrophils or macrophages over 50% possibly suggests a wound age of 12 h or 5 days, and the ratio of MGL-positive myofibroblasts over 60% possibly indicates a wound age of 7 days. Furthermore, in real-time PCR results, the ratio of MGL mRNA expression at 5 days post-injury was shown as >2.54. Besides, no other posttraumatic intervals showed ratios of >2.54. It was worth noting that the tendency of MGL mRNA expression by real-time PCR was almost identical with that of MGL protein expression by Western blotting. Likewise, the ratio of MGL protein expression peaked at 5 days after incision, which was >2.30. Hence, there seems to be an assumption that the ratio of MGL mRNA expression exceeding 2.54 or the ratio of MGL protein expression over 2.30 may indicate a wound age of 5 days. When wound age was <1 day, there was significant difference between 6 and 12 h in real-time PCR result and Western blotting result. Therefore, the present study suggests that the ratio of MGL mRNA and protein expression may be speculated to be more useful parameters for skin wound age determination. According to previous studies [31, 32], various proteins were synthesized after the induction of mRNA, and many cytokine and enzyme mRNAs were almost in accordance with or a little earlier than their proteins. Besides, our previous study demonstrated that it was more appropriate to detect mRNA in early wound age estimation [25]. Thus, detection of mRNA by real-time PCR is more suitable for wound age determination, especially in the early phase of skin wound healing which was usually more sensitive and stable. Accordingly, the combination of real-time PCR, Western blotting, and morphological analysis may minimize the error margin in time calculation with a high degree of accuracy and objectivity in wound age determination.

In conclusion, investigation of expression and distribution of MGL suggests that MGL expressed by neutrophils, macrophages, and myofibrolasts may be involved in modulating levels of 2-AG during the skin-incised wound healing. MGL mRNA, detected by real-time PCR, might be a more sensitive indicator of wound age in forensic wound examination, and it is beyond any doubt that this approach will open up a wide field of wound age estimation for forensic pathology. However, only animal tissue was investigated for MGL as an indicator of wound age in our study. For forensic casework, a further study with actual human samples is necessary.

Acknowledgment This study was financially supported in part by grant for the Doctoral Program funded by Ministry of Education of China (200801590020) and grant funded by National Natural Science Foundation of China (30271347).

References

1. Marrs W, Stella N (2009) Measuring endocannabinoid hydrolysis: refining our tools and understanding. AAPS J 11:307–311
2. Duncan M, Thomas AD, Cluny NL, Patel A, Patel KD, Lutz B, Piomelli D, Alexander SP, Sharkey KA (2008) Distribution and function of monoacylglycerol lipase in the gastrointestinal tract. Am J Physiol Gastrointest Liver Physiol 295:G1255–G1265
3. Puffenbarger RA (2005) Molecular biology of the enzymes that degrade endocannabinoids. Curr Drug Targets CNS Neurol Disord 4:625–631
4. Karlsson M, Reue K, Xia YR, Lusis AJ, Langin D, Tornqvist H, Holm C (2001) Exon–intron organization and chromosomal localization of the mouse monoglyceride lipase gene. Gene 272:11–18
5. Blankman JL, Simon GM, Cravatt BF (2007) A comprehensive profile of brain enzymes that hydrolyze the endocannabinoid 2-arachidonoylglycerol. Chem Biol 14:1347–1356
6. Singer AJ, Clark RA (1999) Cutaneous wound healing. N Engl J Med 341:738–746
7. Guan DW, Ohshima T, Kondo T (2000) Immunohistochemical study on Fas and Fas ligand in skin wound healing. Histochem J 32:85–91

8. Kondo T, Ohshima T (1996) The dynamics of inflammatory cytokines in the healing process of mouse skin wound: a preliminary study for possible wound age determination. Int J Leg Med 108:231–267
9. Dreßler J, Bachmann L, Kasper M, Hauck JG, Müller E (1997) Time dependence of the expression ICAM (CD-54) in human skin wound. Int J Leg Med 110:299–304
10. Hayashi T, Ishida Y, Kimura A, Takayasu T, Eisenmenger W, Kondo T (2004) Forensic application of VEGF expression to skin wound age determination. Int J Leg Med 118:320–325
11. Kondo T, Ohshima T, Eisenmenger W (1999) Immunohistochemical and morphometrical study on the temporal expression of interleukin-1α(IL-1α) in human skin wounds for forensic wound age determination. Int J Leg Med 112:249–252
12. Kondo T, Ohshima T, Mori R, Guan DW, Ohshima K, Eisenmenger W (2002) Immunohistochemical detection of chemokines in human skin wounds and its application to wound age determination. Int J Leg Med 116:87–91
13. Dinh TP, Carpenter D, Leslie FM, Freund TF, Katona I, Sensi SL, Kathuria S, Piomelli D (2002) Brain monoglyceride lipase participating in endocannabinoid inactivation. Proc Natl Acad Sci USA 99:10819–10824
14. Gulyas AI, Cravatt BF, Bracey MH, Dinh TP, Piomelli D, Boscia F, Freund TF (2004) Segregation of two endocannabinoid-hydrolyzing enzymes into pre- and postsynaptic compartments in the rat hippocampus, cerebellum and amygdala. Eur J Neurosci 20:441–458
15. Comelli F, Giagnoni G, Bettoni I, Colleoni M, Costa B (2007) The inhibition of monoacylglycerol lipase by URB602 showed an anti-inflammatory and anti-nociceptive effect in a murine model of acute inflammation. Br J Pharmacol 152:787–794
16. Jhaveri MD, Richardson D, Chapman V (2007) Endocannabinoid metabolism and uptake: novel targets for neuropathic and inflammatory pain. Br J Pharmacol 152:624–632
17. Hohmann AG, Suplita RL, Bolton NM, Neely MH, Fegley D, Mangieri R, Krey JF, Walker JM, Holmes PV, Crystal JD, Duranti A, Tontini A, Mor M, Tarzia G, Piomelli D (2005) An endocannabinoid mechanism for stress-induced analgesia. Nature 435:1108–1112
18. Desroches J, Guindon J, Lambert C, Beaulieu P (2008) Modulation of the anti-nociceptive effects of 2-arachidonoylglycerol by peripherally administered FAAH and MGL inhibitors in a neuropathic pain model. Br J Pharmacol 155:913–924
19. McPartland JM (2008) Expression of the endocannabinoid system in fibroblasts and myofascial tissues. J Bodyw Mov Ther 12:169–182
20. Kondo T (2007) Timing of skin wounds. Leg Med 9:109–114
21. Mori R, Kondo T, Nishie T, Ohshima T, Asano M (2004) Impairment of skin wound healing in beta-1,4-galactosyltransferase-deficient mice with reduced leukocyte recruitment. Am J Pathol 164:1303–1314
22. Oka S, Wakui J, Ikeda S, Yanagimoto S, Kishimoto S, Gokoh M, Nasui M, Sugiura T (2006) Involvement of the cannabinoid CB2 receptor and its endogenous ligand 2-arachidonoylglycerol in oxazolone-induced contact dermatitis in mice. J Immunol 177:8796–8805
23. Facchinetti F, Del Giudice E, Furegato S, Passarotto M, Leon A (2003) Cannabinoids ablate release of TNF alpha in rat microglial cells stimulated with lypopolysaccharide. Glia 41:161–168
24. Jordà MA, Verbakel SE, Valk PJ, Vankan-Berkhoudt YV, Maccarrone M, Finazzi-Agrò A, Löwenberg B, Delwel R (2002) Hematopoietic cells expressing the peripheral cannabinoid receptor migrate in response to the endocannabinoid 2-arachidonoylglycerol. Blood 99:2786–2793
25. Yu TS, Cheng ZH, Li LQ, Zhao R, Fan YY, Du Y, Ma WX, Guan DW (2010) The cannabinoid receptor type 2 is time-dependently expressed during skeletal muscle wound healing in rats. Int J Leg Med 124:397–404
26. Di Marzo V, Bisogno T, De Petrocellis L, Melck D, Orlando P, Wagner JA, Kunos G (1999) Biosynthesis and inactivation of the endocannabinoid 2-arachidonoylglycerol in circulating and tumoral macrophages. Eur J Biochem 264:258–267
27. Walter L, Dinh T, Stella N (2004) ATP induces a rapid and pronounced increase in 2-arachidonoylglycerol production by astrocytes, a response limited by monoacylglycerol lipase. J Neurosci 24:8068–8074
28. Cecchi R (2010) Estimating wound age: looking into the future. Int J Leg Med 124:523–536
29. Kagawa S, Matsuo A, Yagi Y, Ikematsu K, Tsuda R, Nakasono I (2009) The time-course analysis of gene expression during wound healing in mouse skin. Leg Med (Tokyo) 11:70–75
30. Sun JH, Wang YY, Zhang L, Gao CR, Zhang LZ, Guo Z (2010) Time-dependent expression of skeletal muscle troponin I mRNA in the contused skeletal muscle of rats: a possible marker for wound age estimation. Int J Leg Med 124:27–33
31. Ohshima T, Sato Y (1998) Time-dependent expression of interleukin-10 (IL-10) mRNA during the early phase of skin wound healing as a possible indicator of wound vitality. Int J Leg Med 111:251–255
32. Bai R, Wan L, Shi M (2008) The time-dependent expressions of IL-1beta, COX-2, MCP-1 mRNA in skin wounds of rabbits. Forensic Sci Int 175:193–197